Department of Pharmaceutical Sciences[1]; Department of Pharmaceutics and Pharmaceutical Technology[2], Faculty of Pharmacy, The University of Jordan, Amman, Jordan

# Preparation of novel ionotropically crosslinked beads based on alginate-terephthalic acid composites as potential controlled release matrices

R. Al-Otoum[1], S. R. Abulateefeh[2], M. O. Taha[1]

*Received May 11, 2013, accepted June 25, 2013*

*Prof. Dr. Mutasem Omar Taha, Department of Pharmaceutical Sciences, Faculty of Pharmacy, The University of Jordan, Amman 11942, Jordan*
*mutasem@ju.edu.jo*

*Pharmazie 69: 10–18 (2014)* *doi: 10.1691/ph.2014.3122*

Ionotropically crosslinked alginate beads suffer generally from poor drug loading, poor stability in bio-relevant media and hence fast (i.e. uncontrolled) drug release profiles. Therefore, the present work aims at addressing these drawbacks by enhancing the stability of these metal ion-crosslinked alginate complexes *via* the incorporation of terephthalic acid which is proposed to act as a bridging crosslinking aid. In addition to the effect of terephthalic acid, we investigated the effect of curing temperature (4, 25 and 40 °C) and curing cross-linking metal ions (zinc, calcium and aluminum) on the characteristics of the resulting beads, i.e., drug loading and release profiles. Methylene blue (MB) was used as loaded drug model. The resulting beads were chemically and physically probed using infrared spectroscopy and differential scanning calorimetry. Interestingly, all prepared alginate-terephthalate beads (i.e., cured with zinc, calcium and aluminum) illustrated higher MB loadings and accessed controlled release profiles compared to their corresponding terephthalate-free alginate counterparts. Calcium-crosslinked alginate-terephthalate beads illustrated enteric release behavior regardless of their curing temperature. On the other hand, zinc-crosslinked alginate-terephthalate beads accessed enteric-like release profiles when only cured at 40 °C. However, aluminum-crosslinked alginate-terephthalate beads yielded interesting zero order release profiles regardless of their curing temperatures.

## 1. Introduction

Commercial alginates or align are natural polymers extracted from different species of brown algae (Smidsrod and Skjak-Braek 1990). These polymers consist chiefly of the sodium salt of alginic acid, which is a linear copolymer of 1,4-linked mannopyranosyluronic acid and 1,4-linked gulopyranosyluronic acid units, as shown in Fig. 1A (George and Abraham 2006; Shilpa et al. 2003; Raj and Sharma 2003).

Alginic acid has been categorized by the FDA as being generally regarded as safe (GRAS). It is biodegradable and non-toxic when given orally. Therefore, alginate is used extensively in food industry as a thickener, emulsifier and stabilizer (Espevik et al. 1993).

Alginate has been investigated as a carrier material in different controlled release systems including microparticles, nanoparticles or minimatrices (Joshi et al. 2011; Zhang et al. 2010; Moebus et al. 2009; Trandafilovic et al. 2012; Pillay and Fassihi 1999a, Pillay and Fassihi 1999b). Alginate carriers have been used to encapsulate a variety of medicinal agents including protein drugs (Mobus et al. 2012), gene transfection agents (Nograles et al. 2012; Patnaik et al. 2006) and other small molecule drugs such as anti-cancer agents (Nagarwal et al. 2012). Additionally, alginic acid and related derivatives have attracted recent interest in the pharmaceutical field due to their good mucoadhesive properties (Chang et al. 1985; George and Abraham 2006; Schnürch et al. 2001; Gum et al. 1992).

Alginic acid has been reported to form stable complexes with divalent and trivalent metallic cations (e.g., with $Ca^{2+}$, $Zn^{2+}$ or $Al^{3+}$). Alginate-metal gelation can be carried out under extremely mild conditions with non-toxic reactants (Taha et al. 2008; Nokhodchi and Tailor 2004). The gelation and cross-linking of the alginic acid polymeric networks are mainly achieved by exchange of sodium ions from the guluronic acid residues with the divalent cations, and the stacking of these guluronic groups to form the characteristic egg-box structure (Smidsrod and Skjak-Braek 1990).

Calcium-based alginate systems received most attention due to their facile preparation and nontoxic profiles (Lee and Mooney 2012). Still, Ca-alginate beads have two important problems: (i) The loaded drug is usually partially lost during ionotropic curing through leaching via the microporous crosslinked crust of the beads (Liu and Krishnan 1999). (ii) Calcium-alginate beads dissolve completely in phosphate buffered saline solution (pH 7.4) within a short period after a certain lag time (Kikuchi et al. 1997). In fact, calcium-alginate matrices were able to extend the release of chloramphenicol and theophylline only in pure water. On the other hand, drug release proceeded much more rapidly in 0.1 M HCl, simulated gastric fluid (SGF), simulated intestinal fluid (SIF) and 0.1 M NaCl solution. The cross-linking calcium

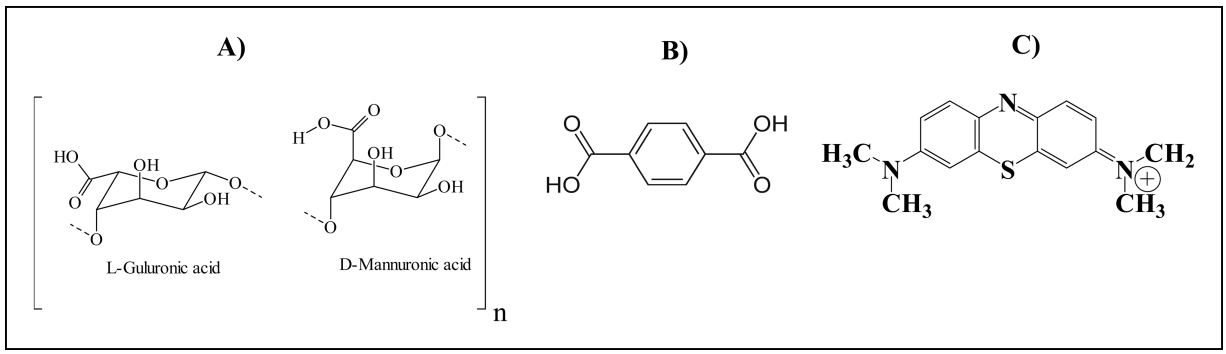


Fig. 1: Chemical structures of A) alginic acid; B) terephthalic acid and C) methylene blue.

ions were rapidly discharged from the matrices in the presence of acid to yield the protonated alginic acid. On the other hand, in NaCl solutions and SIF, calcium ions were partly exchanged by the non-gelling sodium ions or sequestered by phosphate. This caused swelling and, in the latter case, dissolution of the matrices, thus inducing rapid release of the encapsulated drug. Accordingly, it was concluded that calcium alginate minimatrices do not seem applicable as an oral controlled release system, due to their pronounced sensitivity towards the composition of the release medium and the rapid drug release in media of physiological relevance (Ostberg et al. 1994).

These problems prompted several attempts to synthetically modify alginic acid in such a way to enhance the stability of its corresponding complexes with divalent (or trivalent) cations under physiological conditions (Taha and Aiedeh 2000; Aiedeh and Taha 2001; Taha et al. 2005). Moreover, zinc-alginate beads were stabilized during ionotropic crosslinking and in gastric environment by mixing with anionic surfactant sodium lauryl sulfate (SLS) prior to bead formation (Taha et al. 2008).

The continuous interest in developing modified-release formulations combined with the reported drawbacks of metal-crosslinked alginic acid as controlled release delivery system, prompted us to evaluate the possibility of improving the stability of alginic acid-metal complexes via bridging crosslinks based on terephthalic acid (Fig. 1B).

We envisaged that pre-mixing alginate solutions with terephthalic acid molecules should intensify intra-matrix crosslinking by forming additional bridges among metallic centers within the alginate matrix (Fig. 2). Furthermore, the lipophilic aromatic ring of terephthalate can deter water attacks against the alginic carboxylate-metal coordinate bonds, which should further help in stabilizing the composite matrix and, therefore, effectively modify drug delivery. Figure 2 shows a schematic representation of the proposed role of terephthalic acid in alginate-metal crosslinking.

Terephthalic acid is virtually nontoxic and has many industrial, pharmaceutical and medical applications particularly as monomer within interesting polymers and co-polymers (OECD SIDS 2001; Kleerebezem et al. 2005; Mahkam et al. 2006; Mao et al. 2005). Recently, polyethyelene terephthalate was combined with hydroxyapatite to yield composite microfibers that mimic the structure of biological bone (Dimitrievska et al. 2008). Furthermore, poly(ethyleneglycol)-terephthalate/poly(butylenes terephthalate) (PEGT/PBT) multiblock copolymer microspheres were investigated as possible matrix for controlled delivery of small water-soluble drugs (Sohier et al. 2003; Dijkhuizen-Radersma et al. 2002).

We decided to choose methylene blue (MB) as model drug due to its excellent water solubility (3.55 g soluble in 100 mL) (Tuite and Kelly 1993; Tardivo et al. 2004; Via and Magno 2001). In addition, MB has the advantage of being easily analyzable with excellent absorptivity within the visible region (molar absorptivity of 85,000 $M^{-1}$ $cm^{-1}$ at $\lambda_{max}$ of 664 nm) (Fig. 1C). Interestingly, MB was reported to be implemented as model compound for dissolution studies for water soluble drugs (Chavanpatil et al. 2007; Chunder et al. 2007).

## 2. Investigations, results and discussion

### *2.1. Preparation of MB-loaded zinc-crosslinked alginate-terephthalate beads*

Our previous reports have shown excellent coordination qualities of zinc ions to carboxylic acids. For example, zinc-crosslinked chitosan diacetate matrices succeeded in sustaining the release of caffeine in a zero-order manner, while on the other hand, corresponding calcium and aluminum-crosslinked matrices released their caffeine load fairly quickly (Aiedeh

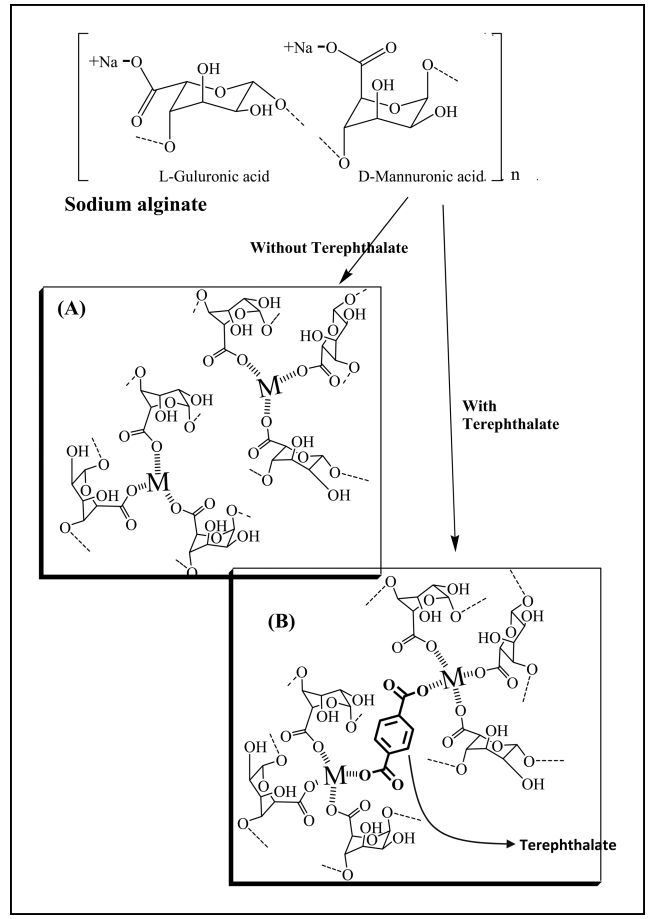


Fig. 2: Schematic representation explaining our hypothesis for incorporating terephthalate into metal (**M**)-crosslinked alginate beads; **(A)** Crosslinking without terephthalate, **(B)** crosslinking with terephthalate.

**Table 1: MB-loaded zinc-crosslinked alginate-terephthalate beads with varying alginate to terephthalate ratios and curing temperatures with the corresponding practical MB loadings**

| Formula | Amount of terephthalate acid (g) | Equivalents ratio[a] (alginate: Terephthalate) | Curing temperature (°C) | Practical MB loading[c] (mg/g beads) |
|---|---|---|---|---|
| F1 | 0 | 1:0 | RT[b] | 9.1 ± 0.3 |
| F2 | 0.8 | 1:1 | RT[b] | 11.7 ± 0.2 |
| F3 | 1.6 | 1:2 | RT[b] | 15.8 ± 0.3 |
| F4 | 0 | 1:0 | 4 | 22.8 ± 0.1 |
| F5 | 0.8 | 1:1 | 4 | 44.7 ± 0.7 |
| F6 | 1.6 | 1:2 | 4 | 41.8 ± 2.1 |
| F7 | 3.2 | 1:4 | 4 | 32.6 ± 0.9 |
| F8 | 0 | 1:0 | 40 | 9.4 ± 0.1 |
| F9 | 0.8 | 1:1 | 40 | 9.4 ± 0.4 |
| F10 | 1.6 | 1:2 | 40 | 16.6 ± 0.7 |
| F11 | 3.2 | 1:4 | 40 | 14.8 ± 0.9 |
| F12 | 4 | 1:5 | 40 | 13.2 ± 0.1 |

[a] Ratio of carboxylic moieties in alginate to terephthalate. Each 5.2 gm sodium alginate contain 0.025 mole carboxylate, i.e., 2.0 gm alginate contain $9.615 \times 10^{-3}$ mole carboxylate.
[b] RT(Room Temperature = 25 ± 2 °C).
[c] Each value represents the average of three loading measurements ± standard deviations.

et al. 2007). Similarly, zinc-crosslinked beads based on alginate/sodium lauryl sulfate composites accessed enteric release behavior, while on the other hand, calcium crosslinking failed completely in modifying drug release from these matrices. The superior release profiles of zinc-crosslinked matrices were attributed to the optimal electrophilic hardness/softness position of zinc ions (Aiedeh et al. 2007; Taha et al. 2008). Therefore, zinc was chosen in the start-up studies to investigate their effect in the preparation of MB loaded alginate-terephthalate beads.
MB-loaded zinc-crosslinked alginate and alginate-terephthalate beads were prepared by dropping a solution of MB, dissolved in an aqueous solution of sodium alginate and varying levels of terephthalic acid (Table 1) into a 10% w/v solution of $ZnSO_4$. The resulting beads were generally dark blue rounded in shape which reduced in size upon drying with an average diameter of ca. 1–2 mm (Fig. 3).

### *2.1.1. MB loading in zinc-crosslinked beads: Effect of terephthalate content and curing temperature*

As shown in Table 1, terephthalate-free zinc-crosslinked alginate beads (F1) exhibited MB loading of 9.1 mg/g. However, incorporation of increasing amounts of terephthalic acids generally accessed higher MB loadings, e.g. 11.7 and 15.8 mg/g for F2 and F3, respectively. A similar trend can be seen for formulas prepared at higher and lower curing temperatures e.g., F4 *vs.* F5 cured at 4 °C and F8 *vs.* F10 cured at 40 °C.
Apparently, this behavior is attributed to the lipophilic nature of the aromatic core of terephthalic acid molecules, which tend to repel water and therefore conserve metal-carboxylate coordinate bonds within the polymeric matrix, i.e. from hydration and dissociation, during curing time, and therefore, reduce MB leaching from immature beads to the curing solution. Moreover, increasing terephthalate content is expected to access polymeric species containing extended bridging terephthalate crosslinks based on two or more hydrophobic terephthalate units, which should show more effective water-repellant action, as schematically illustrated in Fig. 4.
Still, excessively high terephthalate contents seem to be associated with moderate reduction in MB loading, e.g., F5 *vs.* F7 or F10 *vs.* F12. We believe this trend is related to certain salting out effects imposed by higher terephthalate concentrations on soluble MB, such that concentrated terephthalate forces some MB to precipitate out from alginate solution prior to crosslinking.
Table 1 also shows the effect of curing temperature on MB loading within zinc-crosslinked formulas. Clearly from the table, beads formed at 4 °C (i.e., formulas F4-F7) contained higher levels of loaded MB compared to those prepared at 40 °C (i.e. formulas F8-F12). For example, both F7 and F11 have similar amounts of alginate and terephthalate while only differ in the curing temperature (4 and 40 °C, respectively). The former exhibited MB loading of 32.6 mg/g while the latter exhibited MB loading of 14.8 mg/g. Apparently, cooling increases polymeric viscosity within forming beads and therefore reduces MB leaching during ionotropic crosslinking.

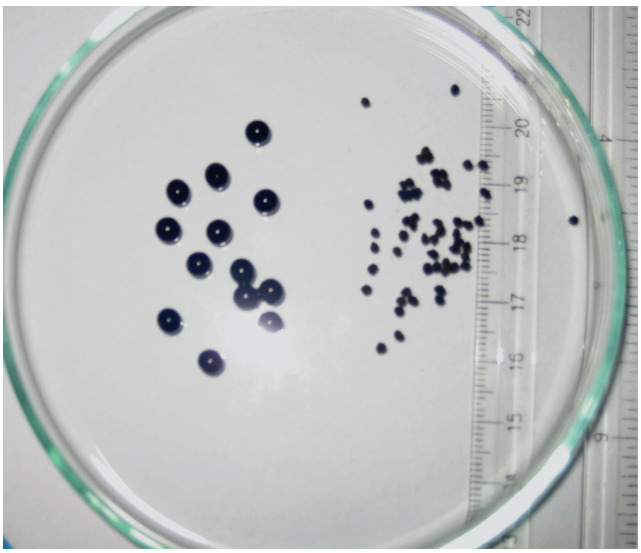

Fig. 3: Wet (left) and dry (right) MB-loaded zinc-crosslinked alginate-terephthalate beads.

### *2.1.2. MB dissolution from different zinc-crosslinked alginate-terephthalate beads formulas*

The dissolution profiles of MB from different bead formulas were studied under simulated gastric conditions (pH = 1.0) followed by simulated intestinal conditions (pH = 6.8). The dissolution media were maintained at 37 °C under sink conditions. Tris buffer was used to generate simulated intestinal pH (6.8) instead of phosphate buffer to avoid the possibility of sequestering the crosslinking metal ions by phosphate. Fig. 5 shows the dissolution profiles of MB from different zinc-crosslinked alginate-terephthalate beads.

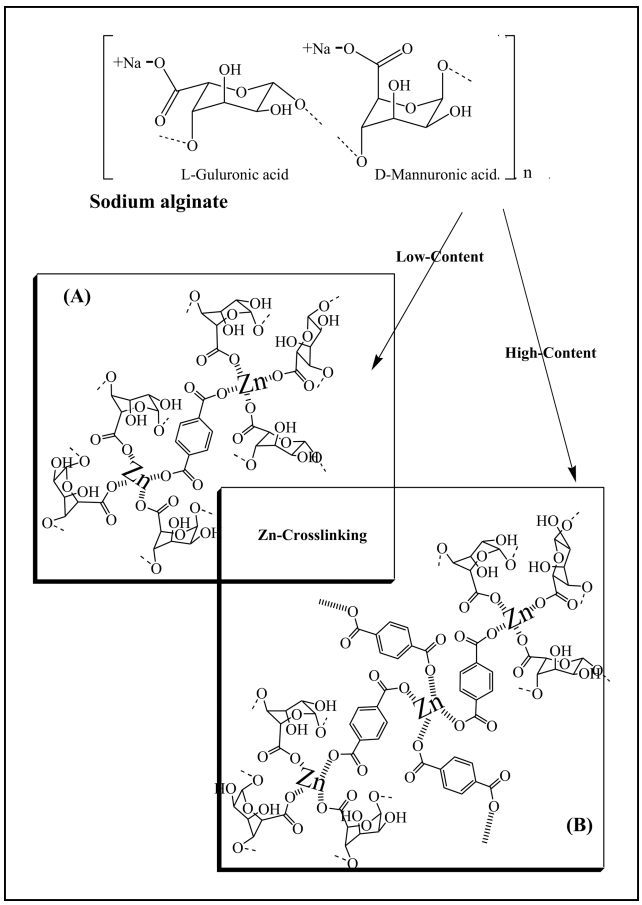


Fig. 4: Schematic representation explaining the probable conduct of terephthalate content on zinc-crosslinked alginate beads; **(A)** With lower terephthalate content (F2), **(B)** with higher terephthalate content (F3).

Terephthalate succeeded in modifying MB release in a manner proportional to its level in the formula. In fact, terephthalate-free zinc-crosslinked alginate beads prepared at RT (F1, Table 1) released > 60% of their MB contents in the simulated gastric pH media. In contrast, terepthhalate-treated zinc-crosslinked alginate beads prepared at the same temperature (F2 and F3, Table 1) illustrated noticeable modified release profiles, i.e., they were able to show significant reductions in MB release under simulated gastric environment. Furthermore, release profiles were rather sensitive to terephthalate contents, such that increasing the amount of terephthalate was accompanied with pronounced reduction in MB release in simulated gastric pH, as evident by comparing formulas F2 *vs.* F3. Similarly, terephthalate-free zinc-crosslinked alginate beads prepared at 40 °C (F8) released

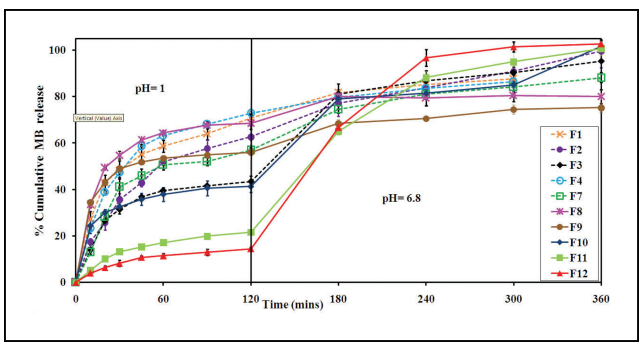


Fig. 5: MB release profiles from different zinc-crosslinked alginate-terephthalate beads (formulas' numbers are as in Table 1). Each point represents the average of three dissolution measurements. Error bars represent the standard deviation of measurements.

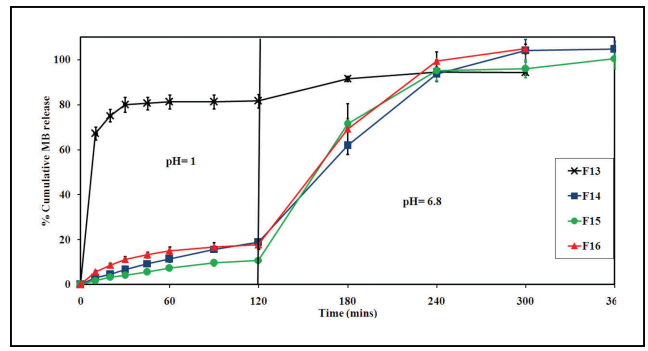


Fig. 6: MB release profiles from different calcium-crosslinked alginate-terephthalate beads (formulas' numbers are as in Table 2). Each point represents the average of three dissolution measurements. Error bars represent the standard deviation of measurements.

their MB contents nearly immediately in the simulated gastric pH media, while, formulas prepared at the same temperature with increasing amounts of terephthalate (i.e. F9-F12) exhibited significant reduction in MB release under simulated gastric pH to the extent of approaching nearly enteric-release behavior (F12). A similar trend was observed with beads prepared at 4 °C (F4 *vs.* F7).

The most acceptable explanation for this intriguing behavior is probably related to the hydrophobic aromatic nature of this compound, particularly after losing its hydrophilic carboxylate groups upon coordination to zinc (or other metallic cations), combined with the favorable bridge-forming *para*-geometry of its dicarboxylic acid moieties. Both factors should help in repelling water attacks on the metal-alginate complexation centers, and therefore, should delay polymeric hydration and subsequent diffusion of loaded model drug molecules. This effect is further enhanced in the presence of higher levels of terepthalate, which should access extended alternating zinc/terephthalate hydrophobic crosslinks bridging alginate scaffolds, as shown in Fig. 3. However, under the basic conditions of simulated intestinal pH, zinc cations seem to exchange terepthalate carboxylates with the abundant hydroxide ions from the medium leading to breakdown of the terepthalate/zinc crosslinks, polymeric hydration and subsequent drug release.

The effect of curing temperature (4 vs. 40 °C) on MB release was also investigated. As shown in Fig. 5, the release profiles are extremely sensitive to curing temperature. For example, comparing the release profiles of formulas cured at 4 °C, e.g., F7, with counterparts cured at 40 °C, e.g., F11 (both with similar contents of terephthalate), suggests a dramatic reduction of MB release under acidic pH in response to higher curing temperature.

Elevated curing temperatures (i.e., 40 °C) seem to increase the degree of zinc-mediated polymeric crosslinking through enhancing the aqueous solubility of crosslinking zinc ions and their diffusablity within the polymeric matrix, thus causing extensive polymeric crosslinking, and consequent formation of thicker crosslinked bead crusts capable of retarding drug release in simulated gastric pH conditions.

### *2.2. Preparation and evaluation of MB-loaded calcium-crosslinked alginate-terephthalate beads*

To probe the effect of crosslinking metal ion on drug loading and release profiles, we switched zinc ions with calcium or aluminum ions. However, we limited our experiments to formulas of higher terephthalate contents (i.e. alginate: terephthalate is 1:4 or 1:5) as they exhibited superior MB loadings and drastically modified MB release profiles in the zinc-based beads. Table 2

**Table 2: MB-loaded calcium-crosslinked alginate-terephthalate beads with varying alginate to terephthalate ratios and curing temperatures with the corresponding practical MB loadings**

| Formula | Amount of terephthalic acid (g) | Equivalents ratio[a] (alginate: Terephthalate) | Curing temperature (°C) | Practical MB loading[b] (mg/g beads) |
|---|---|---|---|---|
| F13 | 0 | 1:0 | 40 | 3.9 ± 0.1 |
| F14 | 3.2 | 1:4 | 40 | 14.8 ± 1.0 |
| F15 | 4.0 | 1:5 | 40 | 16.8 ± 1.1 |
| F16 | 3.2 | 1:4 | 4 | 16.8 ± 0.7 |

[a] Ratio of carboxylic moieties in alginate to terephthalate. Each 5.2 gm sodium alginate contain 0.025 mole carboxylate, i.e., 2.0 gm alginate contain $9.615 \times 10^{-3}$ mole carboxylate.
[b] Each value represents the average of three loading measurements ± standard deviations.

summarizes the different calcium-based formulas, while Fig. 6 shows the corresponding release profiles.

Similar to zinc-crosslinked beads, MB loading in calcium-crosslinked beads was sensitive to terephthalate content: F14 achieved more than three folds increase in MB loading compared to F13. However, MB loading in Ca-crosslinked beads was less sensitive to curing temperature compared to their zinc counterparts. Calcium-crosslinked alginate-terephthalate beads cured at 4 and 40 °C (i.e., F14 and F16 in Table 2) achieved comparable MB loadings of 14.8 and 16.8 mg/g, respectively.

Figure 6 shows MB dissolution profiles from calcium-crosslinked alginate-terephthalate beads. Clearly, calcium-crosslinked beads behaved similar to their zinc-crosslinked counterparts with regard to their sensitivity to terepthalate contents: higher terephthalate content resulted in more sustained MB release (F13 *vs.* F14 and F15). However, calcium crosslinking seemed to be much less sensitive to curing temperature (F14 *vs.* F16). In fact, terephthalate-containing calcium-crosslinked beads illustrated tight enteric behavior regardless to curing temperature.

The temperature-independent profiles of MB loading and release in case of calcium-based beads is probably attributed to the harder, electrostatically explicit calcium ions, compared to their softer zinc counterparts. Hard calcium ions are more suited to form stable coordinate bonds with the hard carboxylate moieties of alginic and terephthalic acids, i.e., compared to zinc ions (Fleming 1996; Aiedeh et al. 2007). The better electrostatic match between calcium and carboxylate ions seems to promote efficient binding and polymeric crosslinking regardless to the temperature-enhancing effects on diffusibility, which was strongly evident with zinc ions.

### *2.3. Preparation and evaluation of MB-loaded aluminum-crosslinked alginate-terephthalate beads*

Similar to zinc- and calcium-crosslinked beads, aluminum-crosslinked beads were sensitive to terephthalate content vis-à-vis MB loading, as shown in Table 3: Aluminum-crosslinked alginate-terephthalate beads (F18 and F19) achieved more than 4 folds increase in MB loading compared to their terephthalate-free counterparts (i.e., F17). Furthermore, MB loading in aluminum-crosslinked beads was also sensitive to curing temperatures: F19 (cured at 4 °C) exhibited statistically significant increase in MB loading compared to F18 (cured at 40 °C) despite their similar compositions.

Moreover, aluminum-crosslinked beads have shown terephthalate-dependent MB release profiles, reminiscent of release behaviors seen in zinc- and calcium-based counterparts (see profiles of F17 *vs.* F18, Fig. 7). Interestingly, however, the combination of aluminum and terephthalate crosslinking (i.e., F18 and F19) yielded apparently time-independent release profiles (Fig. 7). Upon fitting the release data against Korsmeyer–Peppas equation (Korsmeyer et al. 1983; Siepmann and Peppas 2001), it was clear that MB release from F18

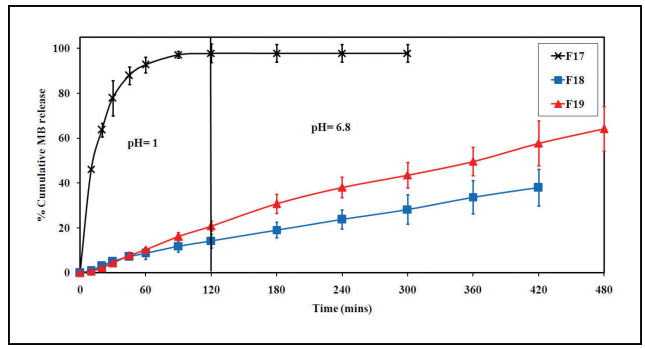


Fig. 7: MB release profiles from different aluminum-crosslinked alginate-terephthalate beads (formulas' numbers are as in Table 3). Each point represents the average of three dissolution measurements. Error bars represent the standard deviation of measurements.

and F19 conform with a Super Case II release approaching a zero order behavior (release exponents are 0.86 and 1.01, respectively, $r^2 = 0.98$).

It remains to be mentioned that MB release from aluminum-crosslinked alginate-terephthalate beads were rather sensitive to curing temperature, such that increasing curing temperature was accompanied with reduction in MB release rates, as evident by comparing formulas F18 and F19 (Fig. 7).

To explain MB loading and release profiles observed for aluminum-based beads, we hypothesize that three factors enhance the crosslinking efficiency of aluminum ions: (i) Electrophilic hardness of aluminum ions (in contrast to soft zinc ions) renders them of optimal match with the hard nucleophilic properties of carboxylate anions of alginates and terephthalate (Fleming 1996; Aiedeh et al. 2007). (ii) The relatively small size of aluminum, compared to calcium (also hard ions), allows efficient diffusion of aluminum ions within the polymeric beads during curing, leading to deeper crosslinking within the inner core of the polymeric beads. (iii) Aluminum ions are capable of forming six coordinate bonds with nucleophilic ligands, which means it can form coordinate complexes with more terephthalate and alginate carboxylate groups with the concomitant result of even more extensive crosslinking and better shielding against hydration water, i.e., compared to calcium and zinc ions, which both have coordination numbers of four (Fleming 1996; Aiedeh et al. 2007; Yokel 2002).

### *2.4. Thermal DSC profiles*

Figure 8 shows the DSC thermograms of zinc-crosslinked alginate and zinc-crosslinked alginate-terephthalate composites compared to corresponding uncrosslinked matrices. Evidently from the figure, all matrices illustrate significant broad bands at 90–100 °C corresponding to evaporation of hydration water within the matrices. However, the DSC trait of zinc-terephthalate composite (trait D in Fig. 8) lacks this band pointing to the extensive hydrophobic nature of this complex.

**Table 3: MB-loaded aluminum-crosslinked alginate-terephthalate beads with varying alginate to terephthalate ratios and curing temperatures with the corresponding practical MB loadings**

| Formula | Amount of terephthalic acid (g) | Equivalents ratio[a] (alginate: Terephthalate) | Curing temperature (°C) | Practical MB loading[b] (mg/g beads) |
|---|---|---|---|---|
| F17 | 0 | 1:0 | 40 | $4.5 \pm 0.3$ |
| F18 | 3.2 | 1:4 | 40 | $17.7 \pm 0.6$ |
| F19 | 3.2 | 1:4 | 4 | $23.2 \pm 0.7$ |

[a] Ratio of carboxylic moieties in alginate to terephthalate. Each 5.2 gm sodium alginate contain 0.025 mole carboxylate, i.e., 2.0 gm alginate contain $9.615 \times 10^{-3}$ mole carboxylate.
[b] Each value represents the average of three loading measurements ± standard deviations.

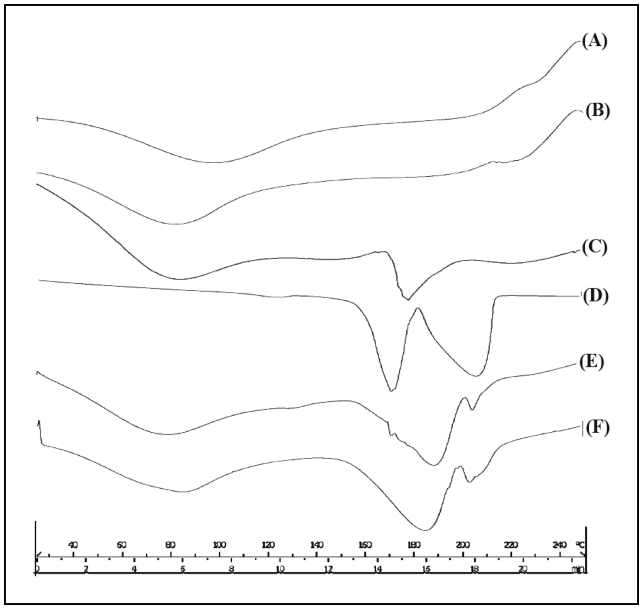


Fig. 8: The DSC traits of **(A**) sodium alginate, **(B)**sodium alginate/sodium terepthalate at 1:2 ratio**, (C)**zinc-crosslinked alginate matrix, **(D)** zinc-terephthalate complex, **(E)**zinc-crosslinked alginate-terepthalate at 1:2 ratio, **(F)** zinc-crosslinked alginate-terepthalate at 1:4 ratio.

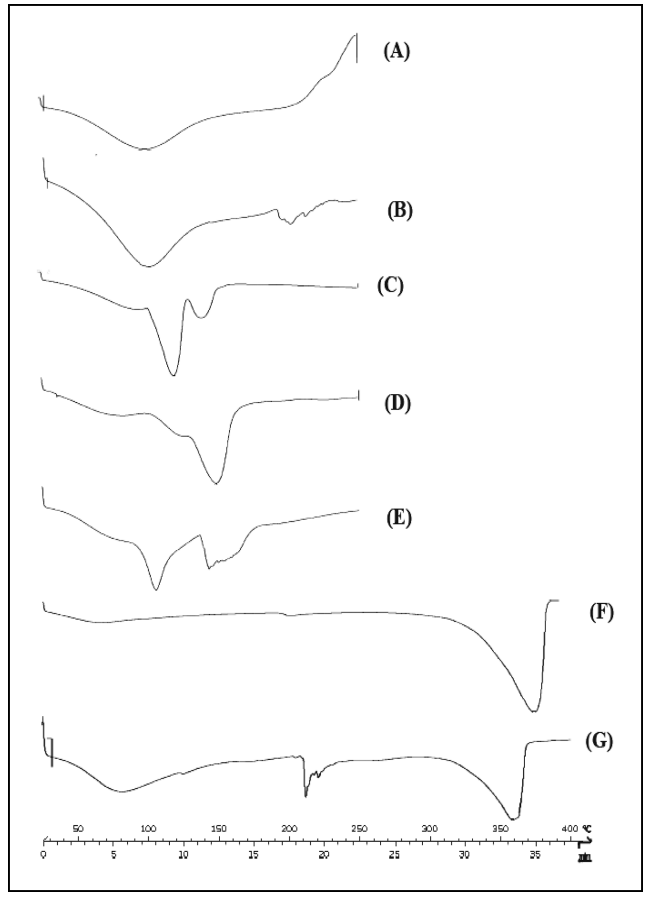


Fig. 9: The DSC traits of **(A**) sodium alginate, **(B)**calcium-crosslinked alginate matrix **(C)** calcium-terephthalate complex **(D)** calcium-crosslinked alginate-terepthalate at 1:4 ratio **(E)**aluminum-crosslinked alginate matrix **(F)** aluminum-terephthalate complex **(G)** aluminum-crosslinked alginate-terepthalate at 1:4 ratio.

Emergence an additional band at *ca*. 180 °C in DSC trait for zinc-crosslinked alginate matrix (C, Fig. 8) compared to the uncrosslinked matrices (A and B, Fig. 8) corresponds to cleavage enthalpies of zinc-carboxylate coordinate bonds within the complex.

The DSC traits of zinc-terephthalate complex (D, Fig. 8) illustrate two distinct bands at *ca.* 170 °C and 210 °C. In contrast, terephthalic acid exhibits sharp melting at 402 °C (O'Neil et al. 2001). These bands correspond to breaking zinc-terephthalate coordinate bonds. We believe the presence of two bands reflects the existence of two closely-related forms of zinc-terephthalate complexes.

The DSC traits of zinc-crosslinked alginate-terephthalate matrices (E and F, Fig. 8) exhibit hybrid bands related to zinc-alginate and zinc-terephthalate complexes. Nevertheless, the second zinc-terephthalate band (at 210 °C) shrank to a little notch in the thermal profile of zinc-crosslinked alginate-terephthalate composites suggesting significant reductions in the levels of the corresponding zinc-terephthalate complex upon the introduction of alginic acid in the formula.

In comparison to zinc, calcium crosslinking seems to be much less pronounced in the DSC traits of calcium-alginate matrices, as shown in Fig. 9 (trait B, minor signals at *ca*. 210 °C). However, upon introducing terephthalic acid, a major broad band emerged at *ca.* 150 °C (D, Fig. 9) corresponding to calcium coordination bonds joining terephthalate and alginate carboxylic acid moieties. This conclusion correlates with the downward shift and splitting of this band in the DSC traits of calcium-terephthalate matrices lacking alginic acid (C, Fig. 9), i.e., lack of alginic acid resulted in less extensive and weaker calcium terephthalate complexes that break at lesser temperature.

However, in comparison to zinc and calcium-crosslinked composites, the thermograms of aluminum-based matrices showed extreme sensitivity to the incorporation of terephthalic acid, as shown in Fig. 9 (traits E, F and G).

Aluminum-alginate complexation yielded broad endothermic band ranging from 140–165 °C (trait E), which is significantly lesser than the corresponding endothermic bands corresponding to zinc- and calcium-crosslinked alginates (*ca.* 180 °C and 200 °C, respectively) suggesting weaker aluminum-alginate coordinate bonds compared to zinc and calcium counterparts. We believe this apparent weakness is not a native property of aluminum-carboxylate coordinate bond, but rather related to hydration of aluminum-carboxylate links within the matrix. This proposition is supported by fact that the hydration band of the aluminum-alginate complex (at 105 °C, trait E) is sharper than corresponding bands in zinc and calcium analogues (both

range 90–100 °C, traits C and B in Figs. 8 and 9, respectively). Sharpness and upward shift of the aluminum-alginate hydration band is indicative of homogenous hydration layers surrounding aluminum-carboyxlate electrostatic centers. Needless to say that extremely hard electrophiles and nucleophiles (e.g. aluminum carboxylate complexes) retain their electrostatic nature upon complexation and maintain high affinity to water molecules (Fleming 1996; Aiedeh et al. 2007; Yokel 2002).

However, upon introducing terephthalic acid, a major broad band emerged at *ca.* 360 °C (trait G, Fig. 9) corresponding to exceptionally strong aluminum-terephthalate coordinate bonds, as can be judged from comparison with the thermogram of aluminum-terephthalate (trait F, Fig. 9). Moreover, addition of terephthalate shifted the aluminum-alginate endothermic band from *ca.* 150 °C to 210 °C (traits E and G, Fig. 9). This intriguing shift is probably related to ejection of hydration water layers surrounding aluminum-alginate coordination centers *via* the hydrophobic nature of complexed terephthalate moieties. This conclusion is supported by disappearance of the sharp hydration band seen in aluminum-alginate thermogram (trait E, Fig. 9) upon adding terephthalate (trait G, Fig. 9). Overall, addition of terephtalic acid strengthened aluminum-alginate complexation and rendered the composite significantly more hydrophobic. This explains the extraordinary release profiles observed for aluminum-alginate-terephthalate composite beads (Fig. 7).

### *2.5. Infrared vibrational profiles*

To probe the impacts of metal crosslinking on alginate and alginate-terephthalate composite matrices, it was decided to evaluate the infrared vibrational spectra of some selected matrices shown in Fig. 10. Unsurprisingly, metal complexation influenced specifically carbonyl stretching vibrations without significantly modifying other bands. Therefore, we will restrict our discussion to this region.

Sodium alginate exhibits significant carbonyl stretching vibration at 1610 $cm^{-1}$ (trait A) corresponding to the carboxylate groups within the polymer. Complexation to zinc (trait B) shifted this band to 1630 $cm^{-1}$ indicative of zinc-carboxylate coordinate bond formation. Zinc complexation is expected to improve the double bond character of the carbonyl groups and therefore strengthen their stretching energies (Williams and Fleming 1997; Taha et al. 2008, Aiedeh et al. 2007). A similar trend is seen upon zinc-terephthalate complexation, i.e., carbonyl stretching vibrations shifted from 1562 $cm^{-1}$ to 1581 $cm^{-1}$ (traits C and D, Fig. 10). Nevertheless, this trend is less obvious in the case of calcium-terephthalate complexation (trait E, *ca.* 1560 $cm^{-1}$), probably because calcium-carboxylate bonding is of lesser coordinate and more electrostatic character compared to zinc-carboxylate bonding (Williams and Fleming 1997; Taha et al. 2008, Aiedeh et al. 2007).

Upon metal complexation, the vibrational profiles of alginate-terephthalate mixtures seem to particularly mirror the behavior of terephthalate, i.e., zinc-crosslinking is apparent at 1583 $cm^{-1}$ (trait F), while calcium-crosslinking caused only subtle change in carbonyl stretching (trait G, 1562 $cm^{-1}$).

On the other hand, aluminum complexation caused drastic changes in carboxylic acid C=O stretching vibrations (traits H, I and J in Fig. 10). In fact, aluminum complexation caused more than 70 $cm^{-1}$ and 120 $cm^{-1}$ upward shifts in the carbonyl stretching bands of alginate and terephthalate, respectively. Undoubtedly, such significant shifts indicate that aluminium-carboxylate bonding is not only electrostatically mediated, but also includes a significant electron transfer component, i.e., formation of strong coordinate bonds.

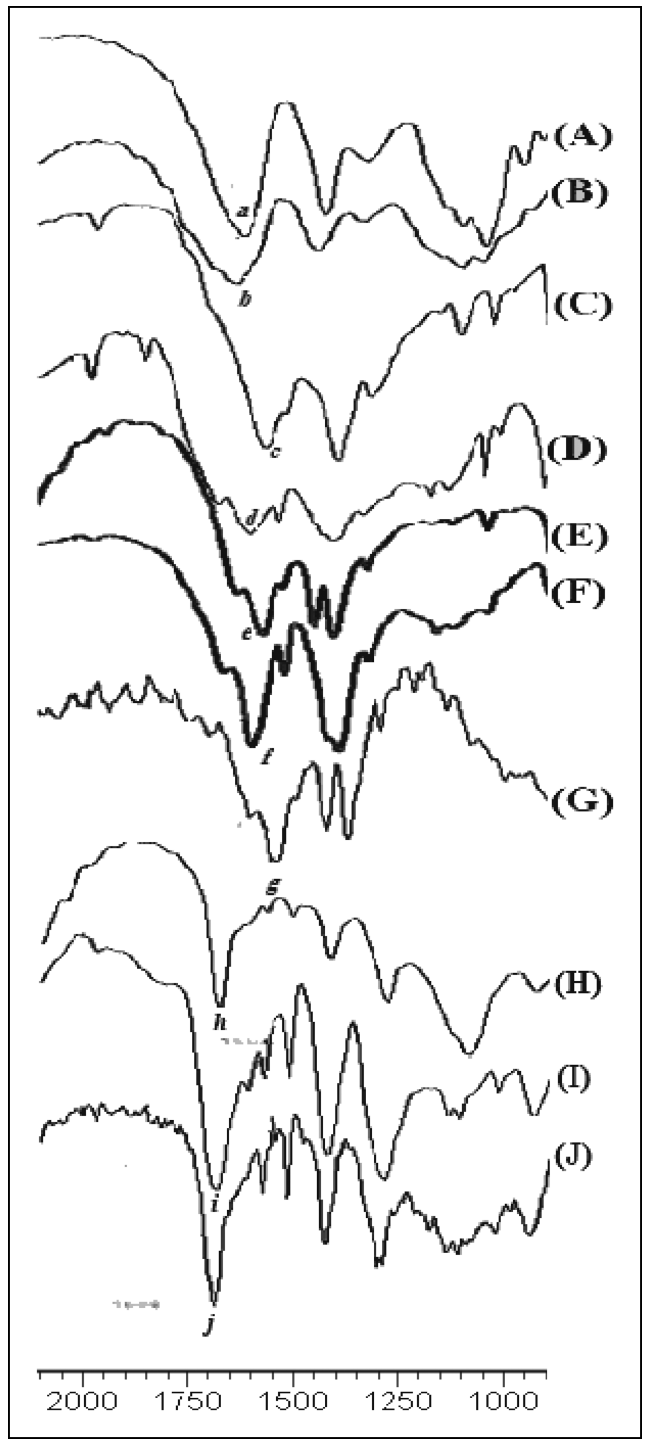


Fig. 10: The IR spectrum of **(A)** sodium alginate, ***a*** = 1610 $cm^{-1}$ **(B)**zinc-crosslinked alginate matrix, ***b*** = 1630 $cm^{-1}$ **(C)** sodium terephthalate, ***c*** = 1562 $cm^{-1}$ **(D)** zinc-terephthalate complex, ***d*** = 1581 $cm^{-1}$ **(E)** calcium-terephthalate complex, ***e*** = 1560 $cm^{-1}$ **(F)** zinc-crosslinked alginate-terepthalate (1:4), ***f*** = 1583 $cm^{-1}$ **(G)**calcium-crosslinked alginate-terepthalate (1:4), ***g*** = 1562 $cm^{-1}$ **(H)**aluminum-crosslinked alginate matrix, ***h*** = 1684 $cm^{-1}$ **(I)** aluminum-terephthalate complex, ***i*** = 1684 $cm^{-1}$ **(J)** aluminum-crosslinked alginate-terepthalate (1:4) ***j*** = 1686 $cm^{-1}$ .

It seems that the excellent electrostatic match (hardness/softness match) between the carboxylate moieties (in particular those of terephthalate) and aluminum ions allows very tight proximity between these oppositely charged ions causing efficient electron transfer from the HOMO orbitals of carboxylate moieties to empty LUMO orbitals on aluminum ions, thus forming rather strong coordinate interactions additional to existing electrostatic interactions. This also explains the drastic effects

aluminum produced on the thermal and release profiles of alginate-terephthalate composites.

### 2.6. Conclusions

Terephthalic acid was found to exert profound concentration and temperature-dependent impacts on the characteristics of zinc-cross-linked alginate beads, such that the combined effects of a particular percentage of terephthalate and warm curing temperature accessed enteric-like release of MB. Calcium-crosslinked beads behaved similar to zinc-crosslinked beads *vis-à-vis* their sensitivity to terepthalate content. However, terephthalate-containing calcium-crosslinked beads illustrated tight enteric behavior regardless to curing temperature. Similar to zinc and calcium-crosslinked beads, aluminum-crosslinked alginate-terephthalate beads exhibited a profound effect of terephthalate content on both MB loading and release. Moreover, these beads illustrated zero-order release behavior regardless to curing temperatures.

## 3. Experimental

### 3.1. Chemicals

The following substances were purchased from corresponding companies (in brackets) and were used as obtained from the manufacturers without further purification. Sodium alginate (Hanawa, Japan), terephthalic acid (The British Drug Houses LTD, England), zinc sulfate heptahydrate (Surechem Products LTD, England), calcium chloride dihydrate (S.d. fine-chem. Ltd, India), aluminum sulfate octadecahydrate (Sigma-Aldrich, USA), tris buffer ultra-pure (Applichem, Germany), hydrochloric acid (Superchem Products LTD, England), sodium acetate trihydrate (S.d. fine-chem. Ltd, India), sodium hydroxide (Scharlan, Spain), methylene blue (BDH, England).

### 3.2. Methods

#### 3.2.1. Formulation of MB-loaded beads

Powdered MB (150 mg) was dissolved gradually in aqueous solution of varying amounts of terephthalic acid (30 ml, amounts of terephthalic acid are as in Tables 1, 2 and 3) and neutralized with equivalent NaOH. The resulting dark blue-colored solution was added to a mechanically-stirred aqueous solution (650 rpm, propeller mixer) of sodium alginate (2.0 gm, 50 ml) to yield a viscous blue solution that was subsequently sonicated for 30 min. Thereafter, the resulting clear solution was slowly dropped, from a 10-cm vertical distance, onto an aqueous solution (100 ml) of the particular curing electrolyte (10 gm%, Tables 1,2 and 3) placed in a shaking water path (GFL1083, Gesellschaft Labortechnik, Germany) under controlled temperature of 4, 25 or 40 °C to yield spherical beads. The resulting beads were left in the electrolyte solution for 30 min. Subsequently, they were filtered, washed with distilled water (2 x 50 ml), and dried at 30 °C over 24 h.

#### 3.2.2. Infrared and thermal characterization of the composite beads

Selected composite beads, in addition to Zn-terephthate, Ca-terephthalate, Al-terephthalate and Na-alginate were characterized by differential scanning calorimetry (DSC) and infrared spectroscopy.

To probe the effect of metal coordination on the polymeric matrix, we prepared and characterized a non-crosslinked composite matrix, i.e., devoid of crosslinking metal and containing Na-alginate/Na-terephthalate in a ratio of 1:2 equivalents, by DSC.

The tested matrices were prepared exactly the same way as their corresponding beads, except that they were generated by adding the curing metal solution to the corresponding vigorously stirred polymer-additive solution without MB at room temperature. The resulting solid whitish masses were filtered, washed with water, and left to dry over few days.

The IR spectra were recorded on an 8400S SHIMADZU IR spectrophotometer using KBr discs. The dried matrices were crushed and KBr discs were prepared from the resulting fine powder. Thermograms were recorded on Mettler TOLEDO Star System. The dried matrices were placed in aluminum pans and heated at a rate of 10 °C/min.

#### 3.2.3. Determination of MB loading in the resulting beads

Total loaded MB per gram beads was calculated as follows; MB-containing beads were crushed, and an accurate weight of the finely crushed beads (0.1 g) was dispersed in NaOH (100 ml, $1 \times 10^{-4}$M) and stirred over two days in shaking water bath at 40 °C**.** The polymeric dispersion was filtered, then 5.0 ml of the solution was withdrawn and diluted to 50.0 ml with NaOH ($1 \times 10^{-4}$M). The concentration of MB was calculated from appropriately drawn calibration plots at $\lambda_{max} = 664$ nm. NaOH solution ($1 \times 10^{-4}$M) was used as a blank.

#### 3.2.4. In vitro release of MB

A rotating basket apparatus (Van Kel 7000) fitted with stainless steel basket was used. In each case, 0.4 g dried beads were placed in the basket and rotated at 100 rpm. Two dissolution media were used over two subsequent stages: 0.1 N HCl media (pH 1.0, 500 ml, 37 °C) for 2 h, then tris buffer media (pH 6.8, 500 ml, 37 °C) for 4 h.

Samples (3 ml) were withdrawn at pre-determined time intervals for analysis of released MB. The withdrawn volume was immediately replaced with an equivalent volume of fresh medium maintained at the same temperature. The absorbance values were measured at $\lambda_{max} = 664$ nm using a Jenway UV–visible spectrophotometer. The corresponding media were utilized as blanks. The concentrations of MB were calculated from appropriately drawn calibration plots (for each pH value).

Acknowledgment: The authors acknowledge the Deanship of Scientific Research at The University of Jordan for their generous funds.

### References

Aiedeh K, Taha MO (1999) Synthesis of chitosan succinate and chitosan phthalate and their evaluation as suggested matrices in orally administered, colon-specific drug delivery systems. Pharmazie 54: 103–107.

Aiedeh K, Taha MO (2001) Synthesis of iron-crosslinked chitosan succinate and iron crosslinked hydroxamated chitosan succinate and their *in vitro* evaluation as potential matrix materials for oral theophylline sustained-release beads. Eur J Pharm Sci 13: 159–168.

Aiedeh K, Taha MO, Al-Hiari Y, Bustanji Y, Alkhatib HS (2007) Effect of ionic crosslinking on the drug release properties of chitosan diacetate matrices. J Pharm Sci 96: 38–43.

Chang H, Park H, Kelly P, Robinson J (1985) Bioadhesive polymers as platforms for oral controlled drug delivery. Synthesis and evaluation of some swelling, water-insoluble bioadhesive polymers. J Pharm Sci 74: 399–405.

Chavanpatil MD, Khdair A, Patil Y, Handa H, Mao G, Panyam J (2007) Polymer-surfactant nanoparticles for sustained release of water soluble drug. J Pharm Sci 96: 3379–3389.

Chunder A, Sarkar S, Yu Y, Zhai L (2007) Fabrication of ultrathin polyelectrolyte fibers and their controlled release properties. Colloids Surf. B Biointerfaces 58: 172–179.

Dijkhuizen-Radersmsn R, Nicolas HM, van deWeert M, Blom M, de Groot K, Bezemer JM (2002) Stability aspects of salmon calcitonin entrapped in poly(ether-ester) sustained release system. Int J Pharm 248: 229–237.

Dimitrievska S, Petit A, Ajji A, Bureau MN, Yahia L (2008) Biocompatibility of novel polymer-apatite nanocomposite fibers. J Biomed Mater Res A 84: 44–53.

Espevik T, Otterlei M, Skjak-Bræk G, Ryan L, Wright SD, Sundan A (1993) The involvement of CD14 in stimulation of cytokine production by uronic acid polymers. Eur J Immunol 23: 255–261.

Fleming I (1996) Frontier orbitals and organic chemical reactions. First edition. London: John Wiley and Sons Ltd. pp 1–32.

George M, Abraham TE (2006) Polyionic hydrocolloids for the intestinal delivery of protein drugs: Alginate and chitosan-a review. J Control Release 114: 1–14.

Gum JR, Hicks JW, Toribara NW, Rothe EM, Lagace RE, Kim YS (1992) The human MUC2 intestinal mucin has cysteine-rich subdomains located both upstream and down stream of its central repetitive region. J Biol Chem 267: 21375–21383.

Joshi A, Solanki S, Chaudhari R, Bahdur D, Aslam M, Srivastava R (2011) Multifunctional alginate microspheres for biosensing, drug delivery and magnetic resonance imaging. Acta Biomater 7**:** 3955–3963.

Kikuchi A, Kawabuchi M, Sugihara M, Sakurai Y, Okano T (1997) Pulsed dextran release from calcium-alginate gel beads. J Control Release 47: 21–29.

Kleerebezem R, Beckers J, Look W, Pol H, Letinga G (2005) High rate treatment of terephthalic acid production wastewater in two-stage anaerobc bioreactor. Biotechnol Bioeng 91: 169–179.

Korsmeyer RW, Gurney R, Doelker E, Buri P, Peppas NA (1983) Mechanisms of solute release from porous hydrophilic polymers. Int J Pharm 15: 25–35.

Lee KY, Mooney DJ (2012) Alginate: Properties and biomedical applications. Prog Polym Sci 37: 106–126.

Liu P, Krishnan TR (1999) Alginate–pectin–poly-l-lysine particulate as a potential controlled release formulation. J Pharm Pharmacol 51: 141–149.

Mahkam M, Doostie L, Siadat SO (2006) Synthesis and characterization of acrylic type hydrogels containing azo derivatives of 5-amino salicylic acid for colon-specific drug delivery. Inflammopharmacology 14: 72–75.

Mao HQ, Shipanova-Kadiyala I, Zhao Z, Dang W, Brown A, Leong KW (2005) Biodegradable poly (terephthalate-co-phosphate)s: synthesis, characterization and drug-release properties. J Biomater Sci Polym Ed 16: 135–161.

Möbus K, Siepmann J, Bodmeir R (2012) Zinc–alginate microparticles for controlled pulmonary delivery of proteins prepared by spray-drying. Eur J Pharm Biopharm 81**:** 121–130.

Möbus K, Siepmann J, Bodmeir R (2009) Alginate–poloxamer microparticles for controlled drug delivery to mucosal tissue. Eur J Pharm Biopharm 72**:** 42–53.

Nagarwal RC, Kumar R, Pandit JK (2012) Chitosan coated sodium alginate–chitosan nanoparticles loaded with 5-FU for ocular delivery: *In vitro* characterization and *in vivo* study in rabbit eye. Eur J Pharm Sci 47**:** 678–685.

Nograles N, Abdullah S, Shamsudin MN, Billa N, Rosli R (2012) Formation and characterization of pDNA-loaded alginate microspheres for oral administration in mice. J Biosci Bioeng 113**:** 133–140.

Nokhodchi A, Tailor A (2004) In situ crosslinking of sodium alginate with calcium and aluminum ions to sustain the release of theophylline from polymeric matrices.;1; Farmaco 59: 999–1004.

Organization for economic cooperation and development, screening information data set OECD SIDS (2001) Terephtalic acid (TPA), France: Paris.

O'Neil MJ, Smith A, Heckelman PE, Obenchain JR, Gallipeau J, Ann R, D'Arecca MA, Budavari S (2001) The Merck Index an encyclopedia of chemicals, drugs, and biologicals, thirteenth edition, New Jersey: Merck Research Laboratories.

Ostberg T, Lund EM, Graffner C (1994) Calcium alginate matrixes for oral multiple unit administration: IV. Release characteristics in different media. Int J Pharm 112: 241–248.

Pillay V, Fassihi R (1999a) *In vitro* release modulation from crosslinked pellets for site-specific drug delivery to the gastrointestinal tract I. Comparison of pH-responsive drug release and associated kinetics. J Control Release 59: 229–242.

Pillay V, Fassihi R (1999b) *In vitro* release modulation from crosslinked pellets for site-specific drug delivery to the gastrointestinal tract II. Physicochemical characterization of calcium-alginate, calcium-pectinate and calcium-alginate-pectinate pellets. J Control Release 59: 243–256.

Raj NKK, Sharma CP (2003) Oral insulin- a perspective. J Biomater Appl 17: 183–196.

Schnürch AB, Kast CE, Richter MF (2001) Improvement in the mucoadhesive properties of alginate by the covalent attachment of cysteine. J Control Release 71: 277–285.

Shilpa SS, Agrawal ARR (2003) Controlled delivery of drugs from alginate matrix. J Macromol Sci Polymer Rev C43: 187–221.

Siepmann J, Peppas NA (2001) Modeling of drug release from delivery systems based on hydroxypropyl methylcellulose (HPMC). Adv Drug Deliv Rev 48: 139 –157.

Smidsrod O, Skjak-Braek G (1990) Alginate as immobilization matrix for cells, Trends Biotechnol 8: 71–78.

Soheir J, Van Dijkhuizen-Radersma R, de Groot K, Bezemer JM (2003) Release of small water-soluble drugs from multiblock copolymer microspheres: a feasibility study. Eur J Pharm Biopharm 55: 221–228.

Taha MO, Aiedeh K (2000) Synthesis of iron-crosslinked hydroxamated alginic acid and its *in vitro* evaluation as a potential matrix material for oral sustained-release beads. Pharmazie 55: 663–667.

Taha MO, Aiedeh KM, Al-Hiari Y, Al-Khatib H (2005) Synthesis of zinc-crosslinked thiolated alginic acid beads and their *in vitro* evaluation as potential enteric delivery system utilizing folic acid as model drug. Pharmazie 60: 736–742.

Taha MO, Nasser W, Ardakani A, Alkhatib H (2008) Sodium lauryl sulfate impedes drug release from zinc-crosslinked alginate beads: switching from enteric coating release into biphasic profile. Int J Pharm 350: 291–300.

Tardivo JP, Del Giglio A, Paschoal LH, Ito AS, Baptista MS (2004) Treatment of melanoma lesions using methylene blue and RL50 light source. Photodiagnosis Photodyn Ther 1: 345–346.

Trandafilović LV, Bozanić D K, Dimitrijević-Branković S, Luyt AS, Djoković V (2012) Fabrication and antibacterial properties of ZnO–alginate nanocomposites. Carbohydr Polym 88**:** 263–269.

Tuite EM, Kelly JM (1993) Photochemical interactions of methylene blue and analogues with DNA and other biological substrates. J Photochem Photobiol B 21: 103–124.

Via LD, Magno SM (2001) Photochemotherapy in the treatment of cancer, Curr Med Chem 8: 1405–1418.

Williams DH, Fleming L (1997) Spectroscopic Methods in Organic Chemistry, (5th ed). London, p. 27–57.

Yokel RA (2002) Aluminum chelation principles and recent advances. Coordin Chem Rev 228: 97–113.

Zhang X, Hui Z, Wan D, Huang H, Huang J, Yuan H, YU J (2010) Alginate microsphere filled with carbon nanotube as drug carrier. Int J Biol Macromol 47: 389–395.